

The excited hadron spectrum in lattice QCD using a new method of estimating quark propagation

C. Morningstar*, A. Bell*, J. Bulava[†], E. Engelson**, J. Foley*, K.J. Juge[‡],
D. Lenkner*, M. Peardon[§], S. Wallace** and C.H. Wong*

**Dept. of Physics, Carnegie Mellon University, Pittsburgh, PA 15213, USA*

[†]*NIC, DESY, Platanenallee 6, D-15738, Zeuthen, Germany*

***Dept. of Physics, University of Maryland, College Park, MD 20742, USA*

[‡]*Dept. of Physics, University of the Pacific, Stockton, CA 95211, USA*

[§]*School of Mathematics, Trinity College, Dublin 2, Ireland*

Abstract. Progress in determining the spectrum of excited baryons and mesons in lattice QCD is described. Large sets of carefully-designed hadron operators have been studied and their effectiveness in facilitating the extraction of excited-state energies is demonstrated. A new method of stochastically estimating the low-lying effects of quark propagation is proposed which will allow reliable determinations of temporal correlations of single-hadron and multi-hadron operators.

Keywords: Lattice QCD, hadron spectroscopy

PACS: 12.38.Gc, 11.15.Ha, 12.39.Mk

To extract excited-state energies in Monte Carlo calculations of lattice QCD, correlation matrices must be evaluated and operators which couple well to the states of interest are crucial. To study a particular state of interest, all states lying below that state must first be extracted, and as the pion gets lighter in lattice QCD simulations, more and more multi-hadron states will lie below the excited resonances. To reliably determine the energies of the multi-hadron states, multi-hadron operators made from constituent hadron operators with well-defined relative momenta will most likely be needed, and the computation of temporal correlation functions involving such operators requires accurately including the low-lying effects of propagation from all spatial sites on one time slice to all sites on another (or the same) time slice. This talk is a progress report on our efforts to study the excited-state spectrum of QCD using the Monte Carlo method: results from our process of selecting optimal single-hadron operators are presented, and a new method of estimating slice-to-slice quark propagators is proposed.

The use of operators whose correlation functions $C(t)$ attain their asymptotic form as quickly as possible is crucial for reliably extracting excited hadron masses. An important ingredient in constructing such hadron operators is the use of smeared fields. Operators constructed from smeared fields have dramatically reduced mixings with the high frequency modes of the theory. Both link-smearing and quark-field smearing must be applied. Since excited hadrons are expected to be large objects, the use of spatially extended operators is another key ingredient in the operator design and implementation. A more detailed discussion of these issues can be found in Ref. [1].

A first glimpse of the nucleon excitation spectrum using two flavors of dynamical quarks was presented in Ref. [2]. Highly excited states for isospin 1/2 baryons were calculated for the first time using lattice QCD with unquenched configurations. Results were obtained for two pion masses: 416(36) MeV and 578(29) MeV. The lowest four energies were reported in each of the six irreducible representations of the octahedral group at each pion mass. Clear evidence was found for a $5/2^-$ state in the pattern of negative-parity excited states. This agrees with the pattern of physical states and spin 5/2 has been realized for the first time in lattice QCD. Note that in this study, only single-particle interpolating operators were used, so the use of *point-to-all* quark propagators was adequate.

A large effort was undertaken during the summer of 2009 to select optimal sets of baryon and meson operators in a large variety of isospin sectors. The following procedure was used. (1) First, operators with excessive intrinsic noise were removed. This was done by examining the diagonal elements of the correlation matrix and discarding those operators whose self-correlators had relative errors above some threshold for a range of temporal separations. (2) Second, pruning within operator types (single-site, singly-displaced, *etc.*) was done based on the condition number of the submatrices $\hat{C}(t = a_t)$, where $\hat{C}_{ij}(t) = C_{ij}(t) / \sqrt{C_{ii}(t)C_{jj}(t)}$ with $C_{ij}(t) = \langle 0 | O_i(t) O_j^\dagger(0) | 0 \rangle$. The condition number was taken to be the ratio of the largest eigenvalue over the smallest eigenvalue. A value near unity is ideal, indicating near orthogonality of the states produced by the action of the operators on the vacuum. Orthogonality

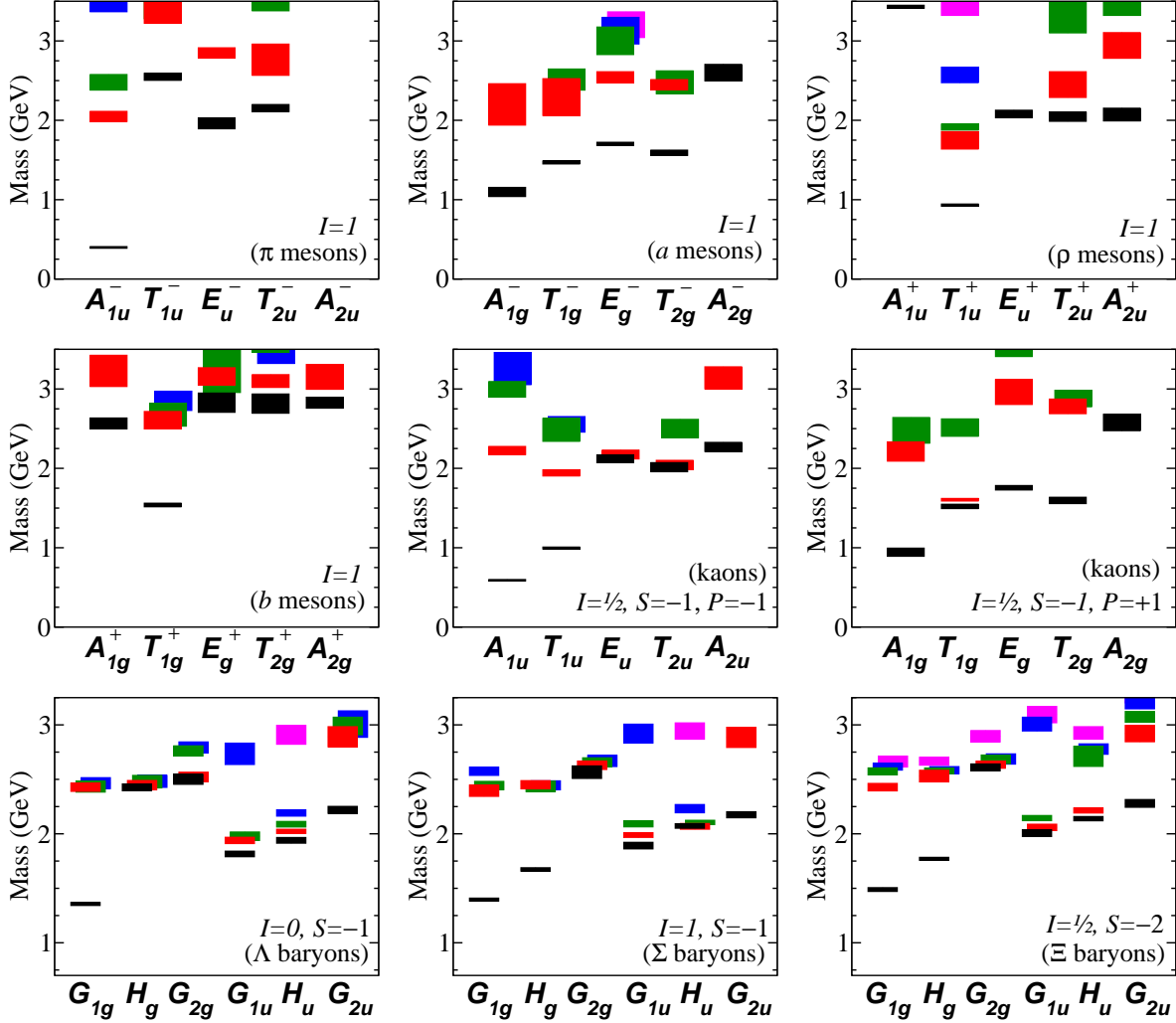


FIGURE 1. Hadron operator selection: low-statistics simulations have been performed to study the hundreds of single-hadron operators produced by our group-theoretical construction. A “pruning” procedure was followed in each channel to select good sets of between six to a dozen operators. The plots above show the stationary-state energies extracted to date from correlation matrices of the finally selected single-hadron operators. Results were obtained using between 50 to 100 configurations on a $16^3 \times 128$ anisotropic lattice for $N_f = 2 + 1$ quark flavors with spacing $a_s \sim 0.12$ fm, $a_s/a_t \sim 3.5$, and quark masses such that $m_\pi \sim 380$ MeV. Each box indicates the energy of one stationary state; the vertical height of each box indicates the statistical error.

prevents noise from creeping into the eigenvalues of the correlation matrix. For each operator type, the set of about six operators which yielded the lowest condition number of the above submatrix was retained. (3) Lastly, pruning across all operator types was done based again on the condition number of the remaining submatrix as defined above. In this last step, the goal was to choose between 8 to 12 operators, keeping two or three of each type, such that a condition number reasonably close to unity was obtained. As long as a good variety of operators was retained, the resulting spectrum seemed to be fairly independent of the exact choice of operators at this stage.

Low-statistics Monte Carlo computations were done to accomplish the above operator selections using between 50 to 100 configurations on a $16^3 \times 128$ anisotropic lattice for $N_f = 2 + 1$ quark flavors with spacing $a_s \sim 0.12$ fm, $a_s/a_t \sim 3.5$, and quark masses such that the pion has mass around 380 MeV. The method described in Ref. [3] was used. Stationary-state energies using the finally selected operator sets are shown in Fig. 1. The nucleon, Δ , Ξ , Σ , and Λ baryons were studied, and light isovector and kaon mesons were investigated. Hundreds of operators were studied, and optimal sets containing eight or so operators in each symmetry channel were found. Future computations will focus solely on the operators in the optimal sets.

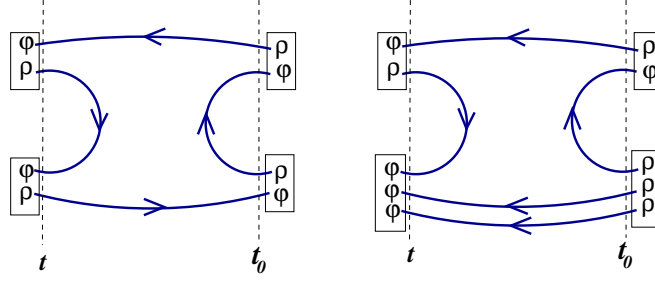


FIGURE 2. Diagrams of multi-hadron correlators that require having ρ noise sources on the later time t . Solution vectors are denoted by φ . (Left) A two-meson correlator. (Right) The correlator of a baryon-meson system.

To study a particular eigenstate of interest in the Monte Carlo method, all eigenstates lying below that state must first be extracted, and as the pion gets lighter in lattice QCD simulations, more and more *multi-hadron* states will lie below the excited resonances. A *good* baryon-meson operator of total zero momentum is typically a superposition of terms having the form

$$B(\mathbf{p}, t)M(-\mathbf{p}, t) = \frac{1}{V^2} \sum_{\mathbf{x}, \mathbf{y}} \varphi_B(\mathbf{x}, t) \varphi_M(\mathbf{y}, t) e^{i\mathbf{p} \cdot (\mathbf{x} - \mathbf{y})},$$

where V is the spatial volume of the lattice, \mathbf{p} is the relative momentum, and $\varphi_B(\mathbf{x}, t)$ and $\varphi_M(\mathbf{y}, t)$ are appropriate localized interpolating fields for a baryon and a meson, respectively. In the evaluation of the temporal correlations of such a multi-hadron operator, it is not possible to completely remove all summations over the spatial sites on the source time-slice using translation invariance. Hence, the need for estimates of the quark propagators from all spatial sites on a time slice to all spatial sites on another time slice cannot be sidestepped. Some correlators will involve diagrams with quark lines originating at the sink time t and terminating at the same sink time t (see Fig. 2), so quark propagators involving a large number of starting times t must also be handled.

Finding better ways to stochastically estimate such slice-to-slice quark propagators for large numbers of quark-line starting times is crucial to the success of our excited-state hadron spectrum project at lighter pion masses. During the past two years, we have been exploring and developing new methods for dealing with such propagators. A first new method, known as distillation[3], was devised in the summer of 2008. We found that direct calculations with this method are feasible on small lattices, but the cost of the computations using this method rises rapidly with the spatial volume. During the past year, the quark-field smearing used in the distillation method was then combined with a stochastic approach to estimating the quark propagators, resulting in a method suitable for large volumes.

The new quark-field smearing scheme, here called Laplacian Heaviside (Laph), has been described in Ref. [3] and is defined by

$$\tilde{\psi}(x) = \Theta \left(\sigma_s^2 + \tilde{\Delta} \right) \psi(x), \quad (1)$$

where $\tilde{\Delta}$ is the three-dimensional covariant Laplacian in terms of the stout-smear gauge field and σ_s is the smearing cutoff parameter. The Heaviside function truncates the sum over Laplacian eigenmodes, restricting the summation to some number N_v of the lowest-lying $-\tilde{\Delta}$ eigenmodes. The number of eigenvectors required increases linearly with the spatial volume of the lattice. In Ref. [3], it was demonstrated that this new smearing method is equally effective at reducing excited-state contamination compared to prior smearing schemes, but this new smearing is advantageous in that it simplifies the computation of slice-to-slice quark propagators.

Random noise vectors η whose expectations satisfy $E(\eta_i) = 0$ and $E(\eta_i \eta_j^*) = \delta_{ij}$ are useful for stochastically estimating the inverse of a large matrix M as follows. Assume that for each of N_R noise vectors, we can solve the following linear system of equations: $MX^{(r)} = \eta^{(r)}$ for $X^{(r)}$. Then $X^{(r)} = M^{-1}\eta^{(r)}$, and $E(X_i \eta_j^*) = M_{ij}^{-1}$ so that a Monte Carlo estimate of M_{ij}^{-1} is given by $M_{ij}^{-1} \approx \lim_{N_R \rightarrow \infty} N_R^{-1} \sum_{r=1}^{N_R} X_i^{(r)} \eta_j^{(r)*}$. Unfortunately, this equation usually produces stochastic estimates with variances which are much too large to be useful. Variance reduction is done by *diluting* the noise vectors[4]. A given dilution scheme can be viewed as the application of a complete set of projection operators $P^{(a)}$. Define $\eta_k^{[a]} = P_{kk'}^{(a)} \eta_{k'}$, and further define $X^{[a]}$ as the solution of $M_{ik} X_k^{[a]} = \eta_i^{[a]}$, then we have

$$M_{ij}^{-1} \approx \lim_{N_R \rightarrow \infty} \frac{1}{N_R} \sum_{r=1}^{N_R} \sum_a X_i^{(r)[a]} \eta_j^{(r)[a]*}. \quad (2)$$

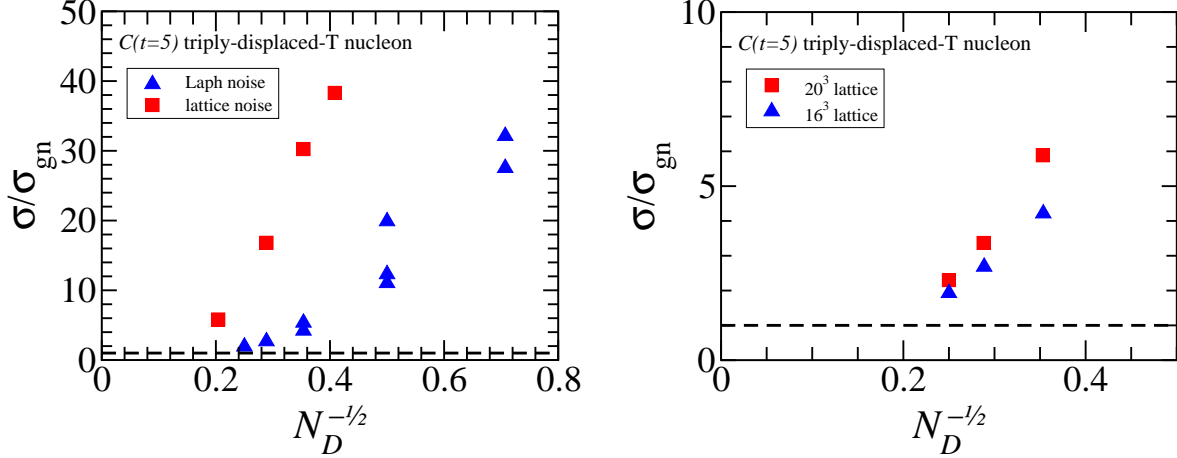


FIGURE 3. (Left) Comparison of the new stochastic Laph method (triangles) with the earlier stochastic method (squares) using noise on the full lattice for the correlator $C(t = 5a_t)$ of a triply-displaced-T nucleon operator on a $16^3 \times 128$ lattice. The vertical scale is the ratio of statistical error σ over the error in the gauge-noise limit σ_{gn} (averaging over the six permutations of the three noises is not done in the results shown in these plots), and in the horizontal scale, N_D is the number of Dirac-matrix inversions per source per quark line. Each point shows an error ratio using a particular dilution scheme. (Right) Comparison of the new Laph stochastic method on 16^3 (triangles) and 20^3 (squares) lattices. The number of Laplacian eigenvectors needed is 32 on the 16^3 lattice and 64 on the 20^3 lattice.

The dilution projections ensure *exact zeros* (zero variance) for our Monte Carlo estimates of many of the off-diagonal elements instead of estimates that are only statistically zero, resulting in a dramatic reduction in the variance of the M^{-1} estimates. The use of Z_4 noise ensures zero variance in our estimates of the diagonal elements. The effectiveness of the variance reduction depends on the projectors chosen.

All previous stochastic methods have introduced noise in the full spin-color-space-time vector space, that is, on the entire lattice itself. However, since we intend to use Laplacian Heaviside quark-field smearing, an alternative is possible: noise vectors ρ can be introduced *only in the Laph subspace*. The noise vectors ρ now have spin, time, and Laplacian eigenmode number as their indices. Color and space indices get replaced by Laplacian eigenmode number. Again, each component of ρ is a random Z_4 variable so that $E(\rho) = 0$ and $E(\rho\rho^\dagger) = I_d$. Dilution projectors $P^{(a)}$ can once again be introduced, but these projectors are matrices in the Laph subspace. Our dilution projectors are products of time dilution, spin dilution, and Laph eigenvector dilution projectors. For each type (time, spin, Laph eigenvector) of dilution, we studied four different dilution schemes. Let N denote the dimension of the space of the dilution type of interest. For time dilution, $N = N_t$ is the number of time slices on the lattice. For spin dilution, $N = 4$ is the number of Dirac spin components. For Laph eigenvector dilution, $N = N_v$ is the number of eigenvectors retained. The four schemes we studied are defined below:

$$\begin{aligned}
 P_{ij}^{(a)} &= \delta_{ij}, & a = 0, & \quad (\text{no dilution}) \\
 P_{ij}^{(a)} &= \delta_{ij} \delta_{ai}, & a = 0, \dots, N-1 & \quad (\text{full dilution}) \\
 P_{ij}^{(a)} &= \delta_{ij} \delta_{a, \lfloor Ki/N \rfloor}, & a = 0, \dots, K-1, & \quad (\text{block-}K) \\
 P_{ij}^{(a)} &= \delta_{ij} \delta_{a, i \bmod K}, & a = 0, \dots, K-1, & \quad (\text{interlace-}K)
 \end{aligned}$$

where $i, j = 0, \dots, N-1$, and we assume N/K is an integer. We use a triplet (T, S, L) to specify a given dilution scheme, where ‘‘T’’ denote time, ‘‘S’’ denotes spin, and ‘‘L’’ denotes Laph eigenvector dilution. The schemes are denoted by 1 for no dilution, F for full dilution, and BK and IK for block- K and interlace- K , respectively. For example, full time and spin dilution with interlace-8 Laph eigenvector dilution is denoted by (TF, SF, LI8).

Introducing noise in this way produces correlation functions with significantly reduced variances, as shown in Fig. 3. Let $C(t)$ denote the correlation function of a representative triply-displaced-T nucleon operator at temporal separation t . Let σ_{gn} represent the statistical error in $C(t = 5a_t)$ using exactly-determined slice-to-slice quark propagators. In other words, σ_{gn} arises solely from the statistical fluctuations in the gauge configurations themselves (the gauge noise). Let σ denote the error in $C(t = 5a_t)$ using stochastic estimates of the quark propagators. The vertical axis in each plot of Fig. 3 is the ratio of the statistical error σ in $C(t = 5a_t)$ over σ_{gn} . Results are shown for a variety of different dilution

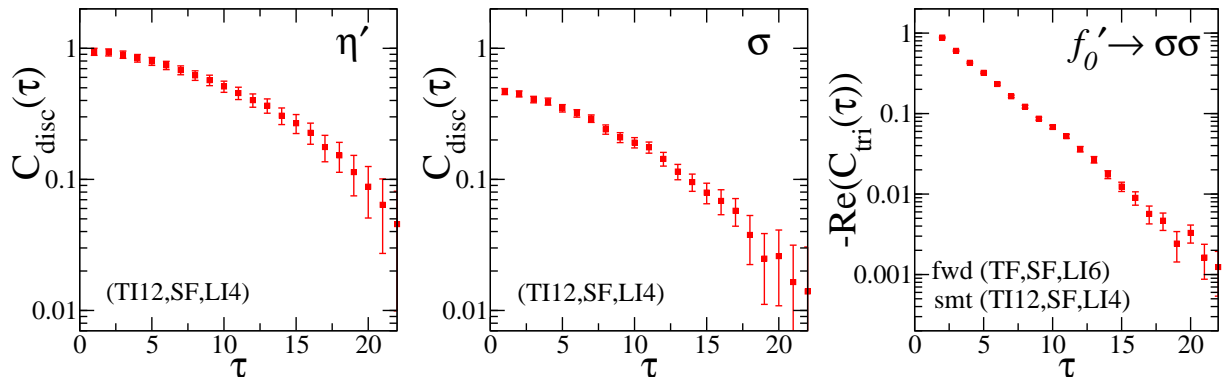


FIGURE 4. Contributions to three correlators involving same-time quark lines evaluated using the new stochastic Laph method. Results are obtained using 99 configs on a small $12^3 \times 96$ anisotropic lattice for quark masses $m_u = m_d = m_s$. Quark lines from the source time t_0 to the sink time t use full time and spin dilution and interlace-6 Laph eigenvector dilution. Quark lines from t to t use interlace-12 time dilution, full spin dilution, and interlace-4 Laph eigenvector dilution. Contributions from only the disconnected diagram are shown for the η' (left) and σ (center) correlators. (Right) The contribution to the $f_0' - \sigma\sigma$ off-diagonal correlator from the two triangle diagrams only is shown.

schemes. In the left plot, the squares show results for dilution schemes with noise introduced in the larger spin-color-space-time vector space, and the triangles show results for different dilution schemes using noise introduced only in the Laph subspace. One sees nearly an order of magnitude reduction in the statistical error.

The volume dependence of this new method was found to be very mild. Calculations on a 16^3 and a 20^3 lattice were carried out and it was found that the ratio $\sigma/\sigma_{\text{gn}}$ of the correlator error over its error in the gauge-noise limit only grew marginally (about 30%) in the larger volume for the *same* number of inversions of the Dirac matrix. Keep in mind that the number of Laplacian eigenvectors needed doubles in going from the smaller to the larger volume. The error ratios for the representative triply-displaced-T nucleon correlator on a 16^3 lattice (triangles) are compared to those from a 20^3 lattice (squares) in Fig. 3.

Different dilution schemes have been explored, and we have found that the combination of full time and spin dilution (one projector for each component) with interlace-8 Laph eigenvector dilution produces a variance near that of the gauge noise limit. Correlation matrix elements evaluated with this method have sufficiently small variances so that diagonalization can be reliably achieved. Using interlace-12 time dilution with full spin and interlace-4 Laph eigenvector dilution, even mixing diagrams between single-hadron and two-hadron states can be accurately estimated, as shown in Fig. 4. The rightmost plot demonstrates that evaluating correlation functions involving our multi-hadron operators will be feasible.

The next steps in our spectrum project are to carry out the operator selection process for single mesons and baryons having non-zero momenta, combine them to form multi-hadron operators, then complete computations of QCD stationary-state energies using, for the first time, both single-hadron and multi-hadron operators. This work was supported by the U.S. National Science Foundation under awards PHY-0510020, PHY-0653315, PHY-0704171 and through TeraGrid resources provided by the Pittsburgh Supercomputer Center, the Texas Advanced Computing Center, and the National Institute for Computational Sciences. MP is supported by Science Foundation Ireland under research grant 07/RFP/PHYF168. The Chroma software suite[5] was used. We thank our colleagues within the Hadron Spectrum Collaboration.

REFERENCES

1. S. Basak, R.G. Edwards, G.T. Fleming, U.M. Heller, C. Morningstar, D. Richards, I. Sato, S. Wallace, Phys. Rev. D **72**, 094506 (2005).
2. J. Bulava, R.G. Edwards, E. Engelson, J. Foley, B. Joo, A. Lichtl, H.-W. Lin, N. Mathur, C. Morningstar, D.G. Richards, S. Wallace, Phys. Rev. D **79**, 034505 (2009).
3. M. Peardon, J. Bulava, J. Foley, C. Morningstar, J. Dudek, R. Edwards, B. Joo, H-W. Lin, D. Richards, K.J. Juge, Phys. Rev. D **80**, 054506 (2009).
4. J. Foley, K.J. Juge, A. O’Cais, M. Peardon, S. Ryan, J. Skullerud, Comput. Phys. Commun. **172**, 145 (2005).
5. R.G. Edwards and B. Joo, Nucl. Phys. B (Proc. Suppl.) **140**, 832 (2005).